

Optical Trapping of an Ion

Ch. Schneider,¹ M. Enderlein,¹ T. Huber,¹ and T. Schaetz^{1,*}

¹Max-Planck-Institut für Quantenoptik, Hans-Kopfermann-Straße 1, D-85748 Garching, Germany

For several decades, ions have been trapped by radio frequency (RF) and neutral particles by optical fields. We implement the experimental proof-of-principle for trapping an ion in an optical dipole trap. While loading, initialization and final detection are performed in a RF trap, in between, this RF trap is completely disabled and substituted by the optical trap. The measured lifetime of milliseconds allows for hundreds of oscillations within the optical potential. It is mainly limited by heating due to photon scattering. In future experiments the lifetime may be increased by further detuning the laser and cooling the ion. We demonstrate the prerequisite to merge both trapping techniques in hybrid setups to the point of trapping ions and atoms in the same optical potential.

I. INTRODUCTION

Scientists in the multifaceted fields working with trapped particles like to cite a 1952 statement by Erwin Schrödinger, one of the founders of quantum mechanics [1]: “[...] it is fair to state that we are not experimenting with single particles, any more than we can raise Ichthyosauria in the zoo.” One year later the first quadrupole mass filter was realized [2, 3] with the first single ion in a radio frequency (RF) trap reported in 1980 [4].

The physical concepts for trapping neutral and charged particles are closely related. Electromagnetic multipole fields act on the charges and dipole moments (e.g., charge distribution), respectively, to provide confining forces on the particles in ponderomotive potentials. The history of trapping neutral particles in dipole traps, however, starts a decade later than ion trapping. The optical dipole force was first considered to provide a confining mechanism in 1962 [5, 6], while the possibility to trap atoms was first proposed by Letokhov [7]. Subsequently, the theoretical background of dipole forces was developed [8, 9], and in 1986 the first optical trapping of neutral atoms was reported by Chu et al. [10]. The first single atoms confined in an optical dipole trap were reported in 1999 [11], again delayed by two decades compared to the first single trapped ion.

One explanation for the delay of trapping neutral particles is that ion traps provide potential depths of the order of several eV $\approx k_B \times 10^4$ K. Optical traps in contrast typically store neutral particles up to 10^{-3} K only. This discrepancy is mainly due to the comparably large Coulomb forces that can be exerted on charged particles. However, the sensitivity to stray electric fields accounts for the paradigm that ions would not be trappable in optical traps. We demonstrate that optical trapping of ions is feasible even in the close vicinity of electrodes and we are able to confine the ion in the dipole potential for hundreds of oscillation periods.

II. EXPERIMENTAL SETUP

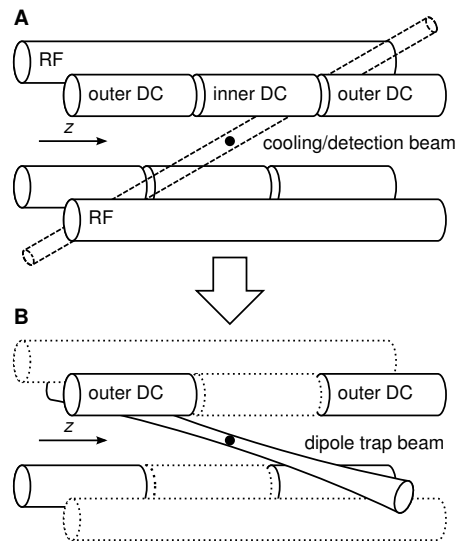


Figure 1: Idealized schemes of the two alternative trapping setups. (A) Initialization of the ion while trapping with the ponderomotive potential of the RF trap and cooling with the Doppler laser. The RF electrodes provide the radial confinement while voltages on the outer DC electrodes prevent the ion from escaping axially. The arrow labeled “z” indicates the axis of the RF trap. (B) Trapping the ion with the dipole trap laser which crosses the axis of the RF trap at an angle of 45° . The ponderomotive potential of the RF trap and the Doppler cooling lasers are turned off.

A single $^{24}\text{Mg}^+$ ion is created by photo-ionization from neutral Mg atoms evaporated from an oven. It is Doppler cooled to a few mK (Doppler cooling limit: 1 mK) in a segmented linear RF trap [12] (Fig. 1A). The ion is loaded into an optical trap by first superimposing the dipole potential provided by a Gaussian laser beam tightly focussed on the ion. Subsequently, the ponderomotive potential of the RF trap is switched off completely by carefully ramping down its RF drive to zero. The dipole potential is kept on for the dipole trap duration T_{dipole} , while the ponderomotive potential of the RF trap is off (Fig. 1B). Afterwards, the ion is transferred back into

*Electronic address: tobias.schaetz@mpq.mpg.de

the RF trap and detected by observing its fluorescence light, if the ion remained trapped in the dipole potential for T_{dipole} . During the entire experiment an additional DC field that is focussing in one dimension is retained to prevent the ion from leaving the dipole trap along the propagation direction of the beam. It is crucial to minimize stray electric fields at the position of the ion and to precisely control the ramp-down of the RF potential.

The dipole trap laser provides a maximal power of around 500 mW at a wavelength of 280 nm. The ultraviolet (UV) beam is generated from a 2 W fiber laser at 1118 nm by two consecutive second harmonic generation (SHG) stages [13]. Currently, we have up to $P_{\text{trap}} = 275$ mW at our disposal for the optical dipole trap. The efficiency is mainly limited by the losses in an acousto-optical modulator used for switching the beam, polarization optics providing a σ^+ -polarization with purity exceeding 1000 : 1, and three telescopes for expanding and cleaning the mode of the beam. The beam has a nearly Gaussian shape with a waist radius of $w_0 = 7$ μm . The frequency of the laser can be detuned up to $\Delta = -2\pi \times 300$ GHz red of the resonance of the $S_{1/2} \leftrightarrow P_{3/2}$ transition of $^{24}\text{Mg}^+$ with a natural line width of $\Gamma = 2\pi \times 41.8$ MHz [14]. According to these parameters we anticipate a depth of the optical potential of $U_0 \approx k_B \times 51$ mK and a maximum force perpendicular to the beam of $F_{\text{rad}} = 2 \times 10^{-19}$ N. The corresponding trapping frequencies at the approximately harmonic bottom of the trap amount to $\omega_{\text{rad}} \approx 2\pi \times 192$ kHz perpendicular and $\omega_k \approx 2\pi \times 2$ kHz in the direction of the beam propagation. The beam crosses the axis of the RF trap at an angle of 45° .

The radial frequencies of the RF trap result from the ponderomotive potential and are initially set to $\omega_{x,y} \approx 2\pi \times 900$ kHz. The radial trap depth can be estimated to $U_{x,y} \approx k_B \times 10\,000$ K from the minimal electrode-ion distance of $R_0 = 0.8$ mm and geometrical considerations. The high voltage for the RF electrodes at a frequency of $\Omega_{\text{RF}} \approx 2\pi \times 56$ MHz is generated by a helical resonator ($1/e$ ring-down time $T_{\text{rd}} = 0.5$ μs). Initially, the axial frequency is tuned to $\omega_z = 2\pi \times 115$ kHz by applying appropriate voltages to the outer DC electrodes (Fig. 1A). The axial frequency is lowered to a value of $\omega_z \approx 2\pi \times 45$ kHz only shortly before each of the next procedures, because the ions are more prone to loss by collisions with residual gas at the corresponding lower axial well depth (~ 0.5 K, see methods).

Before the RF confinement can be substituted by the optical dipole trap, residual static electric fields must be minimized at the position of the ion to reduce their resulting forces to a level smaller than the maximal force of the dipole trap. In our setup there are two main sources of such fields: Dielectrics in proximity of the trap are charged by the photoelectric effect due to stray laser light. Furthermore, each loading process contaminates the trap electrodes which leads to contact potentials (-1.44 V for Mg on Au). The minimization of these fields is achieved by gradually ramping down the RF volt-

age to approximately 15% of the initial amplitude and counteracting the ion's displacement by appropriate voltages applied to all of the DC segments (see Fig. 1) and an additional wire placed below the RF trap. The voltage applied to an inner DC electrode is fine-tuned on the order of few 100 μV corresponding to a residual force in the order of 10^{-20} N at the position of the ion.

We want to emphasize that a stable three-dimensional confinement by exclusively DC voltages is impossible according to Earnshaw's theorem: A DC confinement in one or two dimensions has a defocussing effect in at least one of the remaining dimensions. Stable three-dimensional confinement is possible for RF and DC voltages meeting certain stability criteria (stability diagram [3]). This means that switching off the RF trap by only decreasing the RF voltage is equivalent to running a scan in a RF mass filter and will result in the loss of any ion even before a zero RF voltage is reached. Additionally, there are higher order resonances within the theoretically stable regime because of anharmonicities of the RF field [15]. These effects also have to be considered for the successful transfer of the ion from the ponderomotive potential of the RF trap to the optical dipole trap. Therefore, switching off the RF voltage should be performed fast to avoid excessive heating. The lower limit is imposed by the ring-down of the helical resonator. Currently, 50 μs are chosen to turn off the resonator sufficiently adiabatic.

After the completed initialization, the trapping attempt is performed according to the following protocol:

- switching off the Doppler cooling laser
- switching on the dipole trap laser
- ramping down the ponderomotive potential of the RF trap to effectively zero
- waiting for the dipole trap duration T_{dipole}
- ramping up the ponderomotive potential of the RF trap
- switching off the dipole trap laser
- switching on the Doppler cooling lasers

If the trapping attempt is successful, the ion can be detected by observing its fluorescence light on a CCD camera. The discrimination between successful and unsuccessful trapping attempts has an efficiency of effectively 100%. Trapping attempts according to the above protocol are repeated until the ion is lost.

III. EXPERIMENTAL RESULTS

In Fig. 2 the probability $P(T_{\text{dipole}})$ for an ion to remain in the dipole trap is shown as a function of the trapping duration T_{dipole} . Each data point is determined as the number of successful trapping attempts divided by the total number of attempts with approximately 40 ions (corresponding, e.g., to more than 200 attempts for $T_{\text{dipole}} = 1$ ms). For each ion stray fields were minimized as described above. From the data we calculate a lifetime of $\tau = (1.8 \pm 0.3)$ ms.

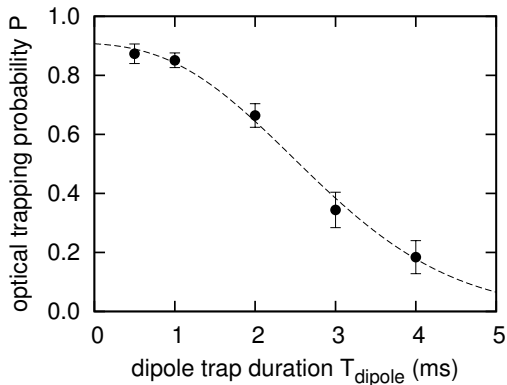


Figure 2: Optical trapping probability $P(T_{\text{dipole}})$ as a function of the trapping duration T_{dipole} : The optical trapping probability is determined as the ratio of successful trapping attempts to the total number of trapping attempts. Each data point represents experiments on ~ 40 ions until each one is lost with statistical errors (except for the point at 500 μs based on 17 ions). The fitted curve (dashed line) is based on a simplistic Markovian heating model (see methods). Experimental parameters: beam waist radius $w_0 = 7 \mu\text{m}$, laser detuning $\Delta = -2\pi \times 275 \text{ GHz}$, laser power $P_{\text{trap}} = 190 \text{ mW}$, axial DC frequency $\omega_z = 2\pi \times 47 \text{ kHz}$, RF switched off

Without cooling, the lifetime in an optical dipole trap is limited by heating. For our experimental parameters with a detuning of $\Delta \approx -6500\Gamma$ recoil heating due to scattering of laser photons [8, 9] poses an upper bound on the lifetime. The experimental parameters yield a Raman scattering rate of $\Gamma_s \approx 860 \text{ ms}^{-1}$ transferring a mean energy of $2 \times E_r \approx 10 \mu\text{K}$ in a single scattering event. With a dipole trap depth of $U_0 \approx k_B \times 38 \text{ mK}$ ($\omega_{\text{rad}} \approx 2\pi \times 165 \text{ kHz}$) for the parameters of Fig. 2 this leads to a lifetime of $\tau_{\text{theo}} \approx 4 \text{ ms}$. This estimate assumes a perfect Gaussian beam, perfect σ^+ -polarization, and zero initial temperature. Furthermore, it does not assume any heating due to the transfer from the RF trap into the dipole trap, due to (fluctuating) residual electric fields, or due to beam pointing instabilities [16]. Since the measured lifetime is not much less than the estimate, we conclude that it is mainly limited by photon scattering.

In Fig. 3 the optical trapping probability $P(P_{\text{trap}})$ is shown as a function of the beam power P_{trap} . The rest of the experimental parameters remains comparable to those in Fig. 2.

We observe that the trapping probability decreases for decreasing P_{trap} (i.e., depth of the dipole potential). Considering only recoil heating and zero initial temperature, the lifetime and thus the optical trapping probability would not depend on the laser power for $P_{\text{trap}} > 0$ in our experiment, because the potential depth as well as the heating rate in the optical dipole trap both scale linearly with P_{trap} . To explain our result we have to take into account, e.g., the non-zero initial temperature and an increasing sensitivity to the quality of the minimization of residual electric fields at lower P_{trap} . The data

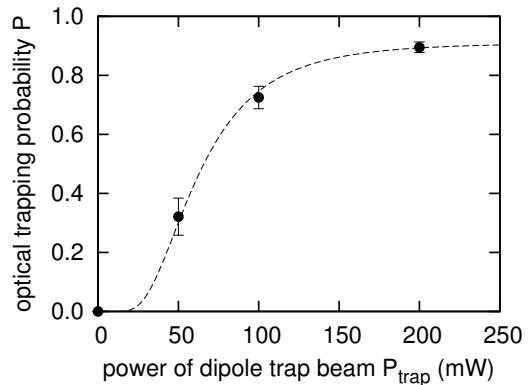


Figure 3: Optical trapping probability $P(P_{\text{trap}})$ as a function of the power of the dipole trap beam P_{trap} : The probability is determined as for Fig. 2, the data points again consider statistical errors only, and the fitted curve (dashed line) is based on the same simplistic Markovian heating model with identical values for the fit parameters (see methods). Experimental parameters: beam waist radius $w_0 = 6.4 \mu\text{m}$, laser detuning $\Delta = -2\pi \times 300 \text{ GHz}$, dipole trap duration $T_{\text{dipole}} = 500 \mu\text{s}$, axial DC frequency $\omega_z = 2\pi \times 41 \text{ kHz}$, RF switched off

point at zero power of the dipole trap beam in Fig. 3 shows that trapping was not achieved without the dipole trap. This emphasizes that there was no relevant residual trapping potential in the experiment.

In both Figs. 2 and 3 the experimental trapping probability reaches a maximum of $P \approx 0.9$. Trapping attempts with a duration $T_{\text{dipole}} \ll 500 \mu\text{s}$ did not exceed this value significantly either. Besides a non-zero initial temperature, there are two additional reasons for that: Firstly, it is due to the fact that the minimum of the dipole potential did not always sufficiently overlap with the position of the ion at turn-off of the RF trap. The beam path from the last SHG stage to the vacuum recipient currently amounts to several meters and the collimated beam is focused by a lens with a focal length of 200 mm onto the ion. This makes the dipole trap beam prone to thermal drifts and shaking caused by convection of the air. Moreover, insufficient minimization of residual static electric fields can give rise to ion loss even at zero T_{dipole} .

IV. OUTLOOK

Our experimental setup leaves room for substantial technical improvements opening up a variety of applications. The main technical challenges are the limited lifetime and coherences of the electronic states. The reduction of the Raman scattering rate Γ_s ($\propto P_{\text{trap}}/\Delta^2$) can be achieved by increasing the detuning Δ . Optical ion trapping might still be feasible even at the reduced potential depth U_0 ($\propto P_{\text{trap}}/\Delta$), if we increased the electrode-ion distance R_0 and therefore reduced the influence of electric potentials and optical stray fields. Yet further improvement is anticipated for larger intensity (and Δ) within an

optical cavity [17] or by larger P_{trap} encouraged by recent laser development that pioneered Raman-amplified systems providing 150 W of laser power at our fundamental wavelength of 1120 nm [18] or 25 W at 589 nm [19], which should be tunable down to 560 nm and allow for efficient SHG. Depending on the intended experiment, using different ion species (e.g., Sr^+ or Ba^+) would permit wavelengths in the visible range. Conventional cooling (Doppler, sideband, Sisyphos cooling) will further enhance the lifetime and cavity cooling, as demonstrated in Ref. [20], might not have to affect the electronic coherence.

Novel applications have been proposed for hybrid setups, combining dipole and ponderomotive RF trap potentials [21, 22]: Superimposing a commensurate optical lattice on the ordered structure of an array of RF traps for individual ions or on an ion crystal frozen within one single RF trap should allow for quantum simulation (QS) experiments of mesoscopic two- or even three-dimensional quantum systems. Dependent on the requirements, the different potentials could also provide confinement in different dimensions. For example, the RF field could provide the radial confinement for a linear chain of ions while a blue detuned optical standing wave could realize the axial confinement within its “dark” lattice sites.

Recently, the combination of a magneto-optical and a RF trap was used to explore cold collisions of atoms and ions [23], however the collision energy was limited by RF-driven micromotion. Conventionally trapped ions were proposed as the ultimate “objective” of a microscope [24] or “read/write head” [21]. For these and most probably further applications it might be advantageous to exploit the charge of trapped particles, but to avoid micromotion. Furthermore, if an ion was loaded into the dipole trap differently, e.g., by photo-ionizing an optically trapped atom, one could avoid electrodes in the vicinity of the ion. Still, electrodes for minimizing residual static electric fields will most probably be required.

Finally, two- and three-dimensional optical lattices might provide an alternative approach for ion trap architectures [12, 21, 25, 26]. One can consider, for example, to implement QS with trapped ions [27, 28] in larger, higher-dimensional systems with the Coulomb force providing long range interaction beyond nearest neighbors. The optical lattice sites would be regularly but sparsely occupied allowing for individual addressability and combining lattices of atoms and ions.

To summarize, we achieved trapping an ion optically even in closest vicinity of electrodes. Additionally, we have shown that hybrid setups, combining optical and RF potentials, are capable to cover the full spectrum of composite confinements—from RF to optical. The lifetime of the ion in the optical dipole trap is limited by photon scattering and is thus expected to be improvable by state of the art techniques.

This work was supported by MPQ, MPG, DFG (SCHA 973/1-4), SCALA and the DFG Cluster of Excellence “Munich Centre for Advanced Photonics”. We thank Hector Schmitz and Robert Matjeschk for preliminary work and Karim Murr, Roman “Ramon” Schmied, and Stephan Dürr for helpful discussions. We also thank Dietrich Leibfried for comments and suggestions on our manuscript and Ignacio Cirac and Gerhard Rempe for their great intellectual and financial support.

Methods: Axial DC Frequency

The loading process contaminates the trap electrodes with Mg from the oven leading to contact potentials (-1.44 V for Mg on Au). A more detailed examination yields an asymmetric axial potential landscape at a frequency of $\omega_z = 2\pi \times 38$ kHz that has a maximum in a distance of approximately $100 \mu\text{m}$ from the position of the ion with a well depth on the order of 0.5 K. In comparison, the outer DC electrodes have a distance of 1.5 mm to the ion. Beyond that maximum the DC fields have a defocussing effect even in axial direction and the ion is pulled out of the trap. Without any contact potentials one would expect a focussing effect of the outer DC electrodes along the z -axis over the complete range of ± 1.5 mm and a well depth which is approximately three orders of magnitude larger.

Methods: Simplistic Markovian Heating Model

The simplistic Markovian heating model assumes a one-dimensional harmonic potential of finite depth $U_0 \propto P_{\text{trap}}$ and a Boltzmann distribution of particle energies. The probability for leaving the trapping potential is then on the order of $\hat{P}(\beta) \approx \exp(-\beta U_0)$ at each attempt with $U_0 = \varepsilon P_{\text{trap}}$ and β defined below; such attempts occur at a frequency Ω_M (not directly related to the dipole trap frequency), giving a temperature-dependent decay rate of $\Gamma_M(\beta) \approx \Omega_M \hat{P}(\beta)$. The differential equation for the probability of having an ion in the dipole trap is $\dot{P}(t) = -P(t)\Gamma_M(\beta(t))$, where we assume the temperature to increase linearly from an initial value: $(k_B\beta(t))^{-1} = T_0 + \gamma P_{\text{trap}}t$. The solution of this differential equation yields the functional form of the fits in Figs. 2 and 3 as the probability $P(T_{\text{dipole}})$ for the ion to remain within the trap after a fixed duration T_{dipole} . The parameters ε/γ , T_0/γ , $\Omega_M/\sqrt{P_{\text{trap}}}$, and a pre-factor C_0 of the function considering improper initialization are optimized in the fits while T_{dipole} and P_{trap} are kept fixed. The deviations of the relevant parameters in Figs. 2 and 3 are within less than 10%. Therefore we have chosen to perform a joint fit for the data.

-
- [1] E. Schrödinger, *Br. J. Philos. Sci.* **3**, 233 (1952).
- [2] W. Paul and H. Steinwedel, *Z. Naturforsch. Teil A* **8**, 448 (1953).
- [3] W. Paul, *Rev. Mod. Phys.* **62**, 531 (1990).
- [4] W. Neuhauser, M. Hohenstatt, P. E. Toschek, and H. Dehmelt, *Phys. Rev. A* **22**, 1137 (1980).
- [5] G. A. Askar'yan, *Zh. Eksp. Teor. Fiz.* **42**, 1567 (1962).
- [6] G. A. Askar'yan, *Sov. Phys. JETP* **15**, 1088 (1962).
- [7] V. S. Letokhov, *JETP Lett.* **7**, 272 (1968).
- [8] J. P. Gordon and A. Ashkin, *Phys. Rev. A* **21**, 1606 (1980).
- [9] J. Dalibard and C. Cohen-Tannoudji, *J. Opt. Soc. Am. B* **2**, 1707 (1985).
- [10] S. Chu, J. E. Bjorkholm, A. Ashkin, and A. Cable, *Phys. Rev. Lett.* **57**, 314 (1986).
- [11] J. Ye, D. W. Vernooy, and H. J. Kimble, *Phys. Rev. Lett.* **83**, 4987 (1999).
- [12] T. Schaetz, A. Friedenauer, H. Schmitz, L. Petersen, and S. Kahra, *J. Mod. Opt.* **54**, 2317 (2007).
- [13] A. Friedenauer, F. Markert, H. Schmitz, L. Petersen, S. Kahra, M. Herrmann, T. Udem, T. W. Hänsch, and T. Schätz, *Appl. Phys. B* **84**, 371 (2006).
- [14] W. Ansbacher, Y. Li, and E. H. Pinnington, *Phys. Lett. A* **139**, 165 (1989).
- [15] A. Drakoudis, M. Söllner, and G. Werth, *Int. J. Mass Spectrom.* **252**, 61 (2006).
- [16] R. Grimm, M. Weidemüller, and Y. B. Ovchinnikov, in *Adv. At. Mol. Opt. Phys.*, edited by B. Bederson and H. Walther (Academic Press, San Diego, 2000), vol. 42, pp. 95–170.
- [17] G. R. Guthöhrlein, M. Keller, K. Hayasaka, W. Lange, and H. Walther, *Nature* **414**, 49 (2001).
- [18] Y. Feng, L. R. Taylor, and D. B. Calia, *Opt. Express* **17**, 23678 (2009).
- [19] Y. Feng, L. R. Taylor, and D. B. Calia, *Opt. Express* **17**, 19021 (2009).
- [20] D. R. Leibbrandt, J. Labaziewicz, V. Vuletić, and I. L. Chuang, *Phys. Rev. Lett.* **103**, 103001 (2009).
- [21] J. I. Cirac and P. Zoller, *Nature* **404**, 579 (2000).
- [22] R. Schmied, T. Roscilde, V. Murg, D. Porras, and J. I. Cirac, *New J. Phys.* **10**, 045017 (2008).
- [23] A. T. Grier, M. Cetina, F. Oručević, and V. Vuletić, *Phys. Rev. Lett.* **102**, 223201 (2009).
- [24] C. Kollath, M. Köhl, and T. Giamarchi, *Phys. Rev. A* **76**, 063602 (2007).
- [25] S. Seidelin, J. Chiaverini, R. Reichle, J. J. Bollinger, D. Leibfried, J. Britton, J. H. Wesenberg, R. B. Blakestad, R. J. Epstein, D. B. Hume, et al., *Phys. Rev. Lett.* **96**, 253003 (2006).
- [26] R. Schmied, J. H. Wesenberg, and D. Leibfried, *Phys. Rev. Lett.* **102**, 233002 (2009).
- [27] D. Porras and J. I. Cirac, *Phys. Rev. Lett.* **92**, 207901 (2004).
- [28] A. Friedenauer, H. Schmitz, J. T. Glueckert, D. Porras, and T. Schaetz, *Nat. Phys.* **4**, 757 (2008).